

Unrestricted Hartree-Fock approach to the insulating behavior of antiferromagnetic CaCuO_2

S. Massidda* and M. Posternak

Institut Romand de Recherche Numérique en Physique des Matériaux (IRRMA), PHB Ecublens, CH-1015 Lausanne, Switzerland

A. Baldereschi

Institut Romand de Recherche Numérique en Physique des Matériaux (IRRMA), PHB Ecublens, CH-1015 Lausanne, Switzerland

and Institut de Physique Appliquée, Ecole Polytechnique Fédérale, PHB Ecublens, CH-1015 Lausanne, Switzerland
(Received 7 July 1992)

Ground-state properties of CaCuO_2 , a parent compound of the high T_c superconductors, are calculated *ab initio* using a LAPW spin-unrestricted Hartree-Fock (UHF) scheme. While CaCuO_2 is a metal within the local-spin density approximation, UHF retains the essential nonlocality of exchange, and predicts a wide gap insulator with an antiferromagnetic moment $\mu \approx 0.8\mu_B$. Results for hypothetical ferromagnetic CaCuO_2 indicate that the insulating character does not depend on the magnetic ordering. The shortcomings of UHF are corrected in part with a simple diagonal-screening model.

One of the peculiarities of the high- T_c superconducting cuprates is the existence of an antiferromagnetic (AFM) insulating phase in the parent compounds (e.g., $\text{Ca}_{1-x}\text{Sr}_x\text{CuO}_2$, La_2CuO_4 , $\text{YBa}_2\text{Cu}_3\text{O}_6$). Although a link between high temperature superconductivity and magnetism has not yet been demonstrated, understanding the magnetic insulating phase is certainly of primary importance in order to obtain a comprehensive picture of high- T_c cuprates.

The AFM behavior is usually ascribed, following the Mott-Hubbard picture,¹ to a large on-site Coulomb repulsion U (the energy to pay in order to doubly occupy a Cu d orbital). A band-theory scheme was proposed by Slater² in the context of the Hartree-Fock formalism. This scheme differs from the Mott-Hubbard one in that it relates the insulating behavior to the AFM spin order. In the cuprates, the persistence of the insulating behavior above the Néel temperature is evidence in favor of the Mott-Hubbard picture.

Calculations on AFM transition-metal oxides and cuprates have been performed within the local-spin-density (LSD) approximation,³ and beyond.⁴ LSD fails to explain the insulating properties of the parent compounds, despite its success in describing, for instance, the Fermi surface of the doped, superconducting materials.⁵ Some model corrections to LSD have also been applied to insulating cuprates,⁶ in order to remedy this deficiency. Recently, Anisimov *et al.*⁷ have done LSD band computations with a model exchange-correlation potential based on the Hubbard scheme, and have obtained the insulating behavior for a number of transition-metal monoxides and the parent compound CaCuO_2 . Closer to the spirit of the present work, but starting from a multiband Hubbard model, Grant and McMahan⁸ have obtained, within

Hartree-Fock theory, realistic values of the superexchange frequency and of the insulating gap in La_2CuO_4 .

The feature which is missing in the LSD approximation and which is necessary for describing Mott-Hubbard insulators is that occupied and empty states should experience different potentials: while an electron sitting in an occupied orbital in a cuprate feels the potential of a d^8 Cu ion, an added electron will feel the potential of a d^9 ion, and the difference between the two energy levels will be the Coulomb repulsion U . When this nonlocality of the self-energy is retained, the insulating behavior can be obtained even within a one-electron approach. We use therefore the conceptually simple self-energy of the (self-consistent) unrestricted Hartree-Fock (UHF) method, which contains the above nonlocality limited to exchange terms. Quantitative errors are hence expected, because of the neglect of the smaller nonlocal effects due to correlation. As a test material, we chose CaCuO_2 , the simplest among the parent cuprates [and recently doped by electrons reaching $T_c \approx 40$ K (Ref. 9)]. We obtain an insulating ground state, with a large gap and an antiferromagnetic moment on the Cu atoms [$\approx 0.8\mu_B$, the experimental value being $\approx 0.51\mu_B$ (Ref. 10)]. Since a relevant question is whether the insulating properties are related to the AFM ordering, we also applied UHF to the ferromagnetic (FM) phase, still obtaining a wide-gap insulator.

The crystallographic structure of CaCuO_2 is simple tetragonal (*st*), with one formula unit per cell and space group D_{4h}^1 . The calculations have been performed in the (AFM) magnetic double-cell, with a body-centered tetragonal (*bct*) space group (D_{4h}^{17}) and using the experimental $\text{Ca}_{0.84}\text{Sr}_{0.16}\text{CuO}_2$ lattice constants $a = 10.32$ a.u., $c = 12.09$ a.u. The spin arrangement assumed¹⁰ was an

tiferromagnetic both in plane and out of plane. FM calculations have also been performed in the *bct* double cell. Both magnetic arrangements have been assumed *a priori*, but in the AFM case the magnitude of the moment was a result of the calculation. In the FM structure, on the other hand, the occupation number was set to be two units larger in the spin-up channel, resulting in a fixed moment of $2\mu_B$ per cell.

The computational method follows the LAPW¹¹ scheme, and will be described in length elsewhere.¹² The HF long-range exchange singularity is treated following Gygi and Baldereschi.¹³ Tests with one and two nonequivalent special points showed convergence of $\approx 0.07\mu_B$ (FM), and $\approx 0.03\mu_B$ (AFM) for the magnetic moments on different atoms, and of ≈ 0.5 eV in the band gaps.

The UHF calculation for the AFM phase uses the zero-moment LSD results as input, and upon iterating produces a magnetic moment on the Cu atoms of $\approx 0.8\mu_B$, to be compared with the experimental value, $\approx 0.51\mu_B$.¹⁰ The neglect of correlation effects is probably the cause of the discrepancy. The oxygens are equivalent by symmetry and carry no total moment. The spin density is quite localized on the Cu sites. In the FM calculation, although the two Cu atoms are not equivalent by the assumed space group, their charges are identical (within $10^{-5} e$). The total charge density is very similar in the AFM and FM calculations.

In Fig. 1 we plot the bands of CaCuO_2 along the Γ -

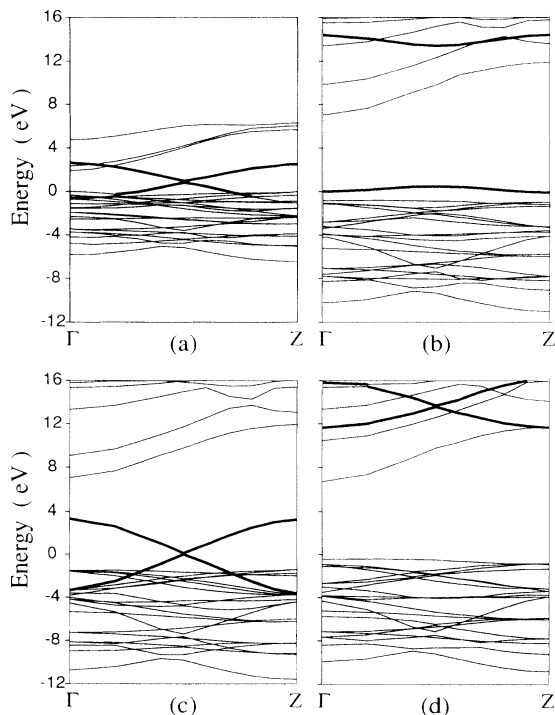


FIG. 1. Energy bands of CaCuO_2 along the Γ - Z direction of the *bct* BZ as calculated within LSD (a), AFM-UHF (b), FM-UHF spin \uparrow (c), and FM-UHF spin \downarrow (d). LSD bands above 6 eV are not shown for clarity.

Z direction of the *bct* Brillouin zone (BZ); in the plot, $Z = (1, 0, 0)2\pi/a$ is equivalent in the *bct* structure to $(0, 0, 1)2\pi/c$. Therefore, this direction gives both in-plane and out-of-plane dispersions. The Γ and $A = (1/2, 1/2, a/2c)2\pi/a$ points of the *st* BZ fold into the *bct* Γ point, while the Z and $M = (1/2, 1/2, 0)2\pi/a$ points fold into the *bct* Z point. Thus, the Γ - Z dispersion contains the information on the relevant in-plane Cu-O *dp* σ bonds. Not shown in the figure are the O $2s$ (valence) bands.

Figure 1 shows the Γ - Z band dispersion for (a) LSD, (b) UHF-AFM (up and down bands are identical), (c) and (d) UHF-FM for spin \uparrow and spin \downarrow , respectively. While LSD gives a semimetal with a nearly zero gap along this line, both the AFM-UHF and FM-UHF calculations give a wide-gap insulator. Also, the total valence bandwidth is much larger in UHF. This is not surprising since the same tendency is observed, e.g., in Si and diamond (40% and 23% larger bandwidth for HF than LSD).¹³

Important differences also occur in the strongly two-dimensional (Γ vs Z symmetry) bands indicated by thick lines and corresponding to the Cu-O *dp* σ^* antibonding states. The behavior of these bands in LSD is similar to that previously found in this,⁶ and other¹⁴ cuprate compounds: the Cu and O states are nonbonding at Γ and strongly antibonding at the *st* A and M points, resulting in a large dispersion.

In the AFM case, these two bands are separated by a large gap of ≈ 13.5 eV, and have little dispersion (≈ 0.45 eV and ≈ 1 eV for the lower and higher bands, respectively). The small dispersion indicates localization of the corresponding orbitals, a feature which is confirmed by the charge density of the two Bloch states at Γ plotted in Fig. 2: out of a nonbonding and of an antibonding state, two completely different molecular orbitals are formed,¹⁵ which are predominantly localized on one of the two Cu atoms, and with a tail extending on the other Cu. By symmetry, the spin \downarrow functions can be obtained from the spin \uparrow ones with a translation bringing Cu(1) into Cu(2). Thus, the spin \uparrow conduction and the spin \downarrow valence states look very much alike, as in Slater's approach.² Analysis of Fig. 2 shows small differences between the valence and conduction states with the same

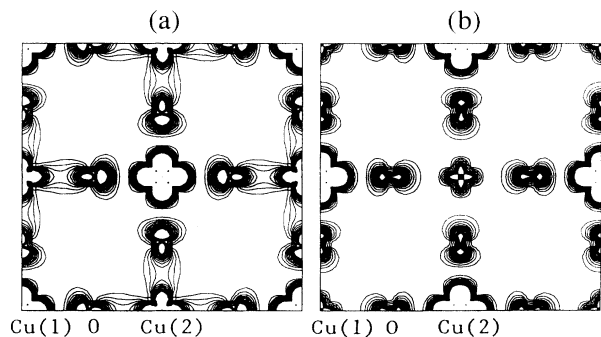


FIG. 2. Electronic charge density for the occupied spin \uparrow (a) and empty spin \uparrow (b) *dp* σ^* states at Γ , as obtained in the UHF-AFM calculation. Contour spacing is $0.002e/a.u.$, and the highest level is $0.028e/a.u.$ ³

spin, accounting for the necessary orthogonalization and for their different symmetries (the two Cu $3d$ orbitals are out of phase in the conduction state, and in phase in the valence one, as seen by the bonding with O $2p$ x , y orbitals). At the Γ - Z midpoint, the lower and higher $d\rho\sigma^*$ states can be decomposed inside muffin-tin spheres as Cu(1) 51%, Cu(2) 3%, O 37% and Cu(1) 1%, Cu(2) 82%, O 13%, respectively. The decomposition depends on the values chosen for the muffin-tin radii, which are larger for Cu ($R = 1.98$ a.u.) than for O ($R = 1.66$ a.u.), but gives an indication of the Cu-O hybridization. While we correctly find the empty $d\rho\sigma^*$ states to be mostly Cu, we get a large Cu component at the valence band top, in contrast with the experimental data in a similar parent compound.¹⁶ This clearly indicates the importance of correlation corrections, which will be discussed later.

In the FM phase, the dispersion of the $d\rho\sigma^*$ bands is larger than in LSD for both spin channels, as expected, the only differences between the two bands being a global shift of about 13.5 eV and a smaller width of the conduction bands.

Only one of the $d\rho\sigma^*$ bands is occupied for each spin in the LSD and AFM calculations, while in the FM case they are both occupied for spin \uparrow and both empty for spin \downarrow . However, the gap between lower- and upper-half bands is vanishing in LSD, and very large in the AFM-UHF calculation. Basically the same separation is found between the center of gravity of occupied spin \uparrow and empty spin \downarrow FM $d\rho\sigma^*$ bands. The origin of this gap is the on-site Coulomb interaction U between electrons with opposite spin. The U value implicit in our calculation is somewhat larger than the one reported in the literature for these compounds, and derived by density-functional calculations ($\approx 7.5 - 10$ eV).^{7,17} The model calculations of Anisimov *et al.*⁷ for CaCuO_2 , and Grant and McMahan⁸ for La_2CuO_4 , give lower values of the $d\rho\sigma^*$ gap in closer agreement with experiment. Correlation terms, which are implicitly taken into account in the above models, are fully neglected in our UHF calculation, and this should explain our large value.⁸ In this respect, the relevance of our calculations is that they provide parameter-free first principles HF results, which can be used as a sound starting point for the inclusion of many-body corrections.

The energy separation at midpoint in the AFM case is related to the nonequivalence (see Fig. 2) of the two Cu atoms in the unit cell (degenerate states are forced to have equal amplitude on the two Cu's), and even more to the occupied vs empty discrimination, deriving from the nonlocality of the exchange interaction. Obviously, the local self-energy used by LSD does not contain this ingredient and the system optimizes the chemical bonding, resulting in a paramagnetic, metallic electronic structure. Similarly, in the FM case, both $d\rho\sigma^*$ states are either filled or empty for a given spin; therefore, the system has no interest in the Cu-Cu disproportionation seen in the AFM case: the two Cu muffin-tin spheres have equal charges, and the states at the Γ - Z midpoint are degenerate within about 10 mRy.

In all our calculations, besides the $d\rho\sigma^*$ states, we find two unoccupied bands with large k_z dispersion (Γ vs Z asymmetry), and a dominant interstitial charac-

ter ($\approx 50\%$ outside muffin-tin spheres). The dispersion of these states is similar in all calculations (including the LSD one), although UHF pushes them up in energy. Within UHF, they are the lowest unoccupied states.

Our UHF results indicate that both AFM and FM ordering lead to a wide-gap insulator in the Mott-Hubbard regime. It should be stressed that these results have been obtained within band theory, and that localization, an essential feature of the Mott-Hubbard insulators, comes out naturally, although use of Bloch wave functions has been made.

While the insulating character originates from the big on-site U term, the antiferromagnetic order is stabilized by weaker interatomic interactions. From our results, we can estimate the superexchange frequency $J = 4t^2/U$,¹⁸ where t is the $d\rho\sigma$ hopping integral. Averaging the widths $W = 2zt$ (where z is the Cu coordination) of the FM $d\rho\sigma^*$ bands for the two spins results in $t = 0.7$ eV, and using $U \approx 13.5$ eV from Fig. 1, we obtain $J \approx 0.15$ eV. Assuming strong-coupling expressions results in a Néel temperature $T_N \approx 900$ K, to be compared with the experimental value $T_N = 537$ K.¹⁰

Despite the prediction of the insulating ground state of CaCuO_2 by UHF, several known shortcomings of this method are found here: much too large energy gaps and incorrect bandwidths are the major problems. The simplest correction scheme is the diagonal COHSEX approximation,¹⁹ where the exchange operator is screened with a static diagonal dielectric function. Since this function is not known for CaCuO_2 , we take as a model¹³ $\epsilon(q) = (q^2 + \alpha^2)/(q^2 + \alpha^2/\epsilon_\infty)$, where $\epsilon_\infty = 5$ is the $\text{La}_{2-x}\text{Sr}_x\text{CuO}_4$ dielectric constant,²⁰ and $\alpha = 0.45$ a.u. preserves unscreened the short-range Coulomb interaction. The results are displayed in Fig. 3 for the AFM phase, and show a significant (and almost rigid) lowering of all the conduction states, which brings

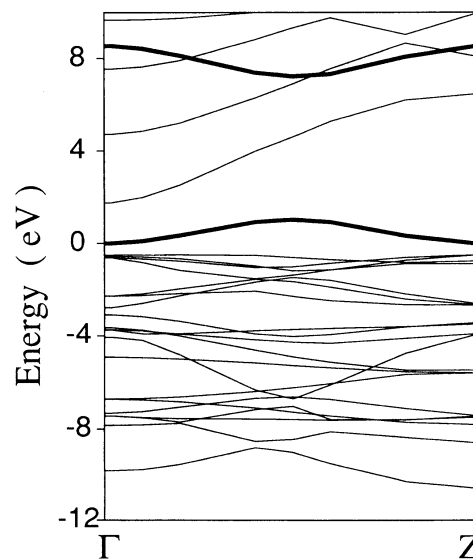


FIG. 3. Energy bands of AFM CaCuO_2 along the Γ - Z direction of the bct BZ, calculated within the diagonal COHSEX approximation, as explained in the text.

the optical gap in much closer agreement with experiment (1.5 eV).²¹ The valence bands remain nearly unchanged. This is consistent with the results found in *s-p* materials.^{13,19} The optical gap is between the Cu-O $dp\sigma^*$ valence states and the interstitial-like conduction states. To our knowledge, there is no experimental evidence either in favor or against this result for CaCuO₂. The gap between the $dp\sigma^*$ half bands is decreased to ≈ 8 eV, and the moment to $0.7\mu_B$. Also, the lower and higher $dp\sigma^*$ bandwidths increase to ≈ 1 and ≈ 1.3 eV, respectively. Upon increasing (not self-consistently) the inverse screening length α to 0.9 a.u., the above bandwidths become, respectively, ≈ 1.4 and ≈ 1.7 eV, with a gap among them of ≈ 3.6 eV, in the direction of a more pronounced metallic behavior.

Considering that the polarizabilities of Cu and O are very much different from each other, large local-field effects can be anticipated in CaCuO₂. They are not included in our diagonal COHSEX scheme, and very likely

they will produce substantial changes in the atomic-orbital contributions to band states, possibly leading to an enhancement of the O character at the valence top, as experiment indicates in a similar parent compound.¹⁶ Also, the relative ordering of conduction bands could be affected by local-field effects. These features can be handled provided one has very detailed and precise information on the response functions of the material. Unfortunately, a first-principle calculation of the dynamical dielectric matrix of CaCuO₂ is at present prohibitively time consuming.

We are grateful to R.M. Martin, T.M. Rice, M. Schlüter, and J. Weber for useful comments. It is a pleasure to acknowledge many stimulating discussions with A.K. McMahan. This work was supported by the Swiss National Science Foundation (Grant No. 30-272.90). The computations were performed in part at ETH-CSCS (Centro Svizzero di Calcolo Scientifico).

*Present address: Centro Ricerca, Sviluppo e Studi Superiori in Sardegna (CRS4), P.O. Box 488, I-09124 Cagliari, Italy.

¹For a review, see N.F. Mott and Z. Zinnamon, *Rep. Prog. Phys.* **33**, 881 (1970); B.H. Brandow, *Adv. Phys.* **26**, 651 (1977).

²J.C. Slater, *Phys. Rev.* **82**, 538 (1951).

³See, for instance, K. Terakura *et al.*, *Phys. Rev. B* **30**, 4734 (1984), and references therein.

⁴A. Svane and O. Gunnarsson, *Europhys. Lett.* **7**, 171, (1988); *Phys. Rev. Lett.* **65**, 1148 (1990); M.R. Norman, *Phys. Rev. B* **44**, 1364 (1991); B. Szpunar and V.H. Smith, *Physica B* **163**, 29 (1990).

⁵See *Proceedings of the Workshop on the Fermiology of High-T_c Superconductors* (Argonne National Laboratory, Argonne, Illinois, 1991); *J. Phys. Chem. Solids* **52**, No. 11/12 (1991).

⁶D. Singh *et al.*, *Physica B* **163**, 470 (1990); L.F. Mattheiss, *Phys. Rev. B* **40**, 2217 (1989).

⁷V.I. Anisimov *et al.*, *Phys. Rev. B* **44**, 943 (1991); *Phys. Rev. Lett.* **68**, 345 (1992).

⁸B. Grant and A.K. McMahan, *Phys. Rev. Lett.* **66**, 488 (1991); (private communication).

⁹M.G. Smith *et al.*, *Nature (London)* **351**, 549 (1991).

¹⁰D. Vaknin *et al.*, *Phys. Rev. B* **39**, 9122 (1989).

¹¹H.J.F. Jansen and A.J. Freeman, *Phys. Rev. B* **30**, 561 (1984).

¹²M. Posternak, S. Massidda, and A. Baldereschi, *Bull. Am. Phys. Soc.* **36**, 570 (1991); (unpublished).

¹³F. Gygi and A. Baldereschi, *Phys. Rev. B* **34**, 4405 (1986).

¹⁴See, for instance, J. Yu *et al.*, *Physica C* **152**, 273 (1989), and references therein.

¹⁵The projections of the AFM $dp\sigma^*$ states at Γ onto the corresponding LSD states (nonbonding and antibonding) amount to about 90% and 95% for the lower and higher Γ states, respectively. The remaining fraction comes from states at lower energy.

¹⁶C.T. Chen *et al.*, *Phys. Rev. Lett.* **66**, 104 (1991).

¹⁷A.K. McMahan, J.F. Annett, and R.M. Martin, *Phys. Rev. B* **42**, 6268 (1990); M.S. Hybertsen, M. Schlüter, and N.E. Christensen, *ibid.* **39**, 9028 (1989).

¹⁸P.W. Anderson, *Solid State Phys.* **14**, 99 (1963).

¹⁹L. Hedin, *Phys. Rev.* **139**, A769 (1965).

²⁰J. Orenstein *et al.*, *Phys. Rev. B* **36**, 729 (1987).

²¹Y. Tokura *et al.*, *Phys. Rev. B* **41**, 11 657 (1990).